

1 **CCL18 signaling from tumor-associated macrophages activates**
2 **fibroblasts to adopt a chemoresistance-inducing phenotype**

3

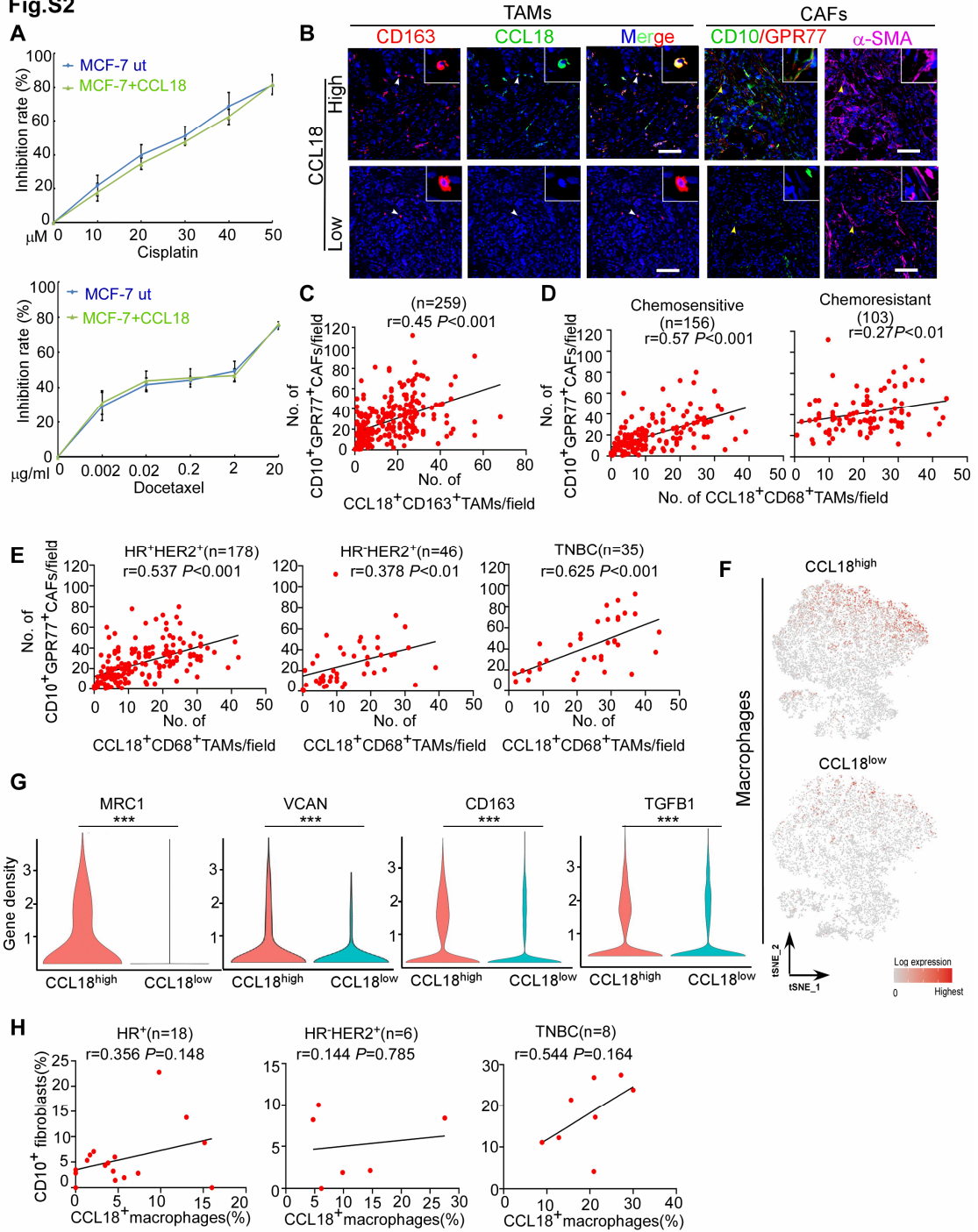
4 Wenfeng Zeng^{1,2,3,#}, Lixiong Xiong^{4,#}, Wei Wu^{1,2,3,#}, Shunrong Li^{1,2,3}, Jiang Liu^{1,2,3},
5 Linbing Yang^{1,2,3}, Liyan Lao^{1,2,3}, Penghan Huang^{1,2,3}, Mengmeng Zhang⁵, Huiping
6 Chen^{1,2,3}, Nanyan Miao^{1,2,3}, Zhirong Lin^{1,2,3}, Zifei Liu^{1,2,3}, Xinyu Yang^{1,2,3}, Jiayi
7 Wang^{1,2,3}, Pei Wang^{1,2,3}, Erwei Song^{1,2,3}, Yandan Yao^{1,2,3*}, Yan Nie^{1,2,3*}, Jianing
8 Chen^{1,2,3*}, Di Huang^{1,2,3*}

9

15 **A**, Representative images of immunofluorescent staining of α -SMA, CD10 and GPR77
16 in the pre-treatment breast cancer biopsies of chemosensitive (n=3) and chemoresistant
17 (n=3) patients. Scale bars, 50 μ m. **B**, Flow cytometric analysis for CD10 and GPR77
18 in primary normal NBFs, MSCs, pericytes, adipocytes, epithelial cells and endothelial
19 cells treated with chemoresistant or chemosensitive tumor CM. **C**, Quantification of
20 Fig.1B: relative α -SMA, FAP, CD10 and GPR77 protein levels in NBFs treated with
21 chemoresistant (n=3) or chemosensitive (n=3) tumor CM was quantified using Image
22 J. Protein levels were normalized to GAPDH. **D**, Quantification of Fig.1C: mean
23 fluorescence intensity (MFI) of CD10 and GPR77 in NBFs treated with chemoresistant
24 (n=3) or chemosensitive (n=3) tumor CM was quantified using Flowjo. **E**, QRT-PCR
25 for ACTA2, FAP, COL1A1, COL3A1, CD10, GPR77, IL-6 and IL-8 in NBFs treated
26 with chemoresistant (n=3) or chemosensitive (n=3) tumor CM. **F**, ELISA for IL-6, IL-
27 8 and CCL18 levels in the CM of chemoresistant (n=3) and chemosensitive tumors
28 (n=3). **G-H**, QRT-PCR(**G**) and mean fluorescence intensity (**H**) for CD10 and GPR77
29 in NBFs treated with chemosensitive tumor CM or chemoresistant tumor CM added
30 without or with neutralizing antibodies against IL6, IL8 or CCL18.
31 Data expressed as mean \pm SEM, *P<0.05, **P < 0.01 compared with chemosensitive
32 tumor CM by two-tailed Student's t test (**F**). Data expressed as mean \pm SEM, *P< 0.05,
33 **P < 0.01, ***P < 0.001 compared with untreated NBFs (Ctrl) by two-tailed one-way
34 ANOVA with Dunnett's multiple comparison test (**C-E**, **G-H**).

35

Fig.S2



36

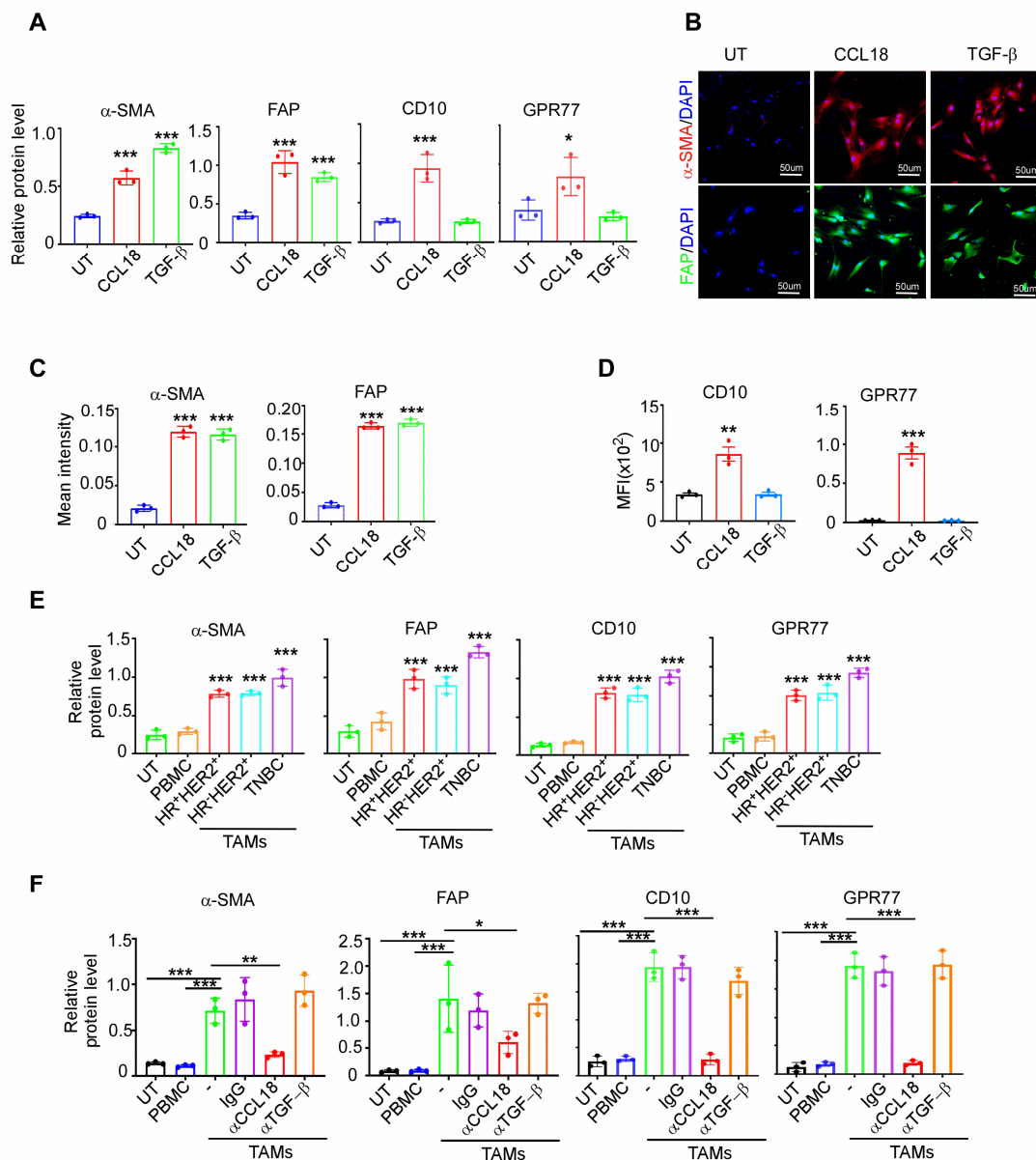
37 **Figure S2. The intratumoral accumulation of CCL18⁺ tumor-associated**
 38 **macrophages is associated with the abundance of CD10⁺GPR77⁺ CAFs and**
 39 **chemoresistance, related to Figure 2**

40 **A, The growth inhibition rate of cisplatin (up) or docetaxel (down) on MCF-7 cells**
 41 **treated without or with CCL18 (n=3). Data expressed as mean \pm SEM, P > 0.1 by two-**

42 tailed Student's t test. **B**, Representative images of immunofluorescent staining of
43 CD163, CCL18, CD10, GPR77 and α -SMA in serial sections of breast cancer samples
44 with high or low CCL18 expression (n=259). Scale bars, 50 μ m. The arrowheads denote
45 the area of higher-magnification images shown in the top-right corner. **C**, The
46 correlation between the abundance of CD10⁺GPR77⁺ CAFs and CD163⁺CCL18⁺
47 TAMs in breast cancer samples. The Pearson's correlation coefficient *r* value and *P*
48 values were determined by two-tailed Pearson correlation coefficient test (n=259). **D-**
49 **E**, Stratification analysis of the correlation between the abundance of CD10⁺GPR77⁺
50 CAFs and CD68⁺CCL18⁺ TAMs in breast tumors with different chemotherapeutic
51 responses (**D**) and molecular subtypes(**E**). HR, hormone receptor. HER2, human
52 epidermal growth factor receptor-2. TNBC, triple negative breast cancer. The Pearson's
53 correlation coefficient *r* value and *P* values were determined by two-tailed Pearson
54 correlation coefficient test. **F**, t-SNE layout of CCL18 expression in divided CCL18^{high}
55 and CCL18^{low} patients from pancancer TME blueprint and GEO: GSE161529. **G**,
56 Violin plots indicating the expression of MRC1, VCAN, CD163 and TGFB1 in
57 macrophages of CCL18^{high} or CCL18^{low} patients. ****P* < 0.001 compared with
58 CCL18^{low} patients by Student's t test. **H**, The correlation between the abundance of
59 CD10⁺fibroblasts and the infiltration of CCL18⁺ macrophages in breast cancer with
60 different molecular subtypes based on scRNA-seq transcriptomes from GEO:
61 GSE161529. The Pearson's correlation coefficient *r* value and *P* values were
62 determined by two-tailed Pearson correlation coefficient test.

63

Fig.S3



64

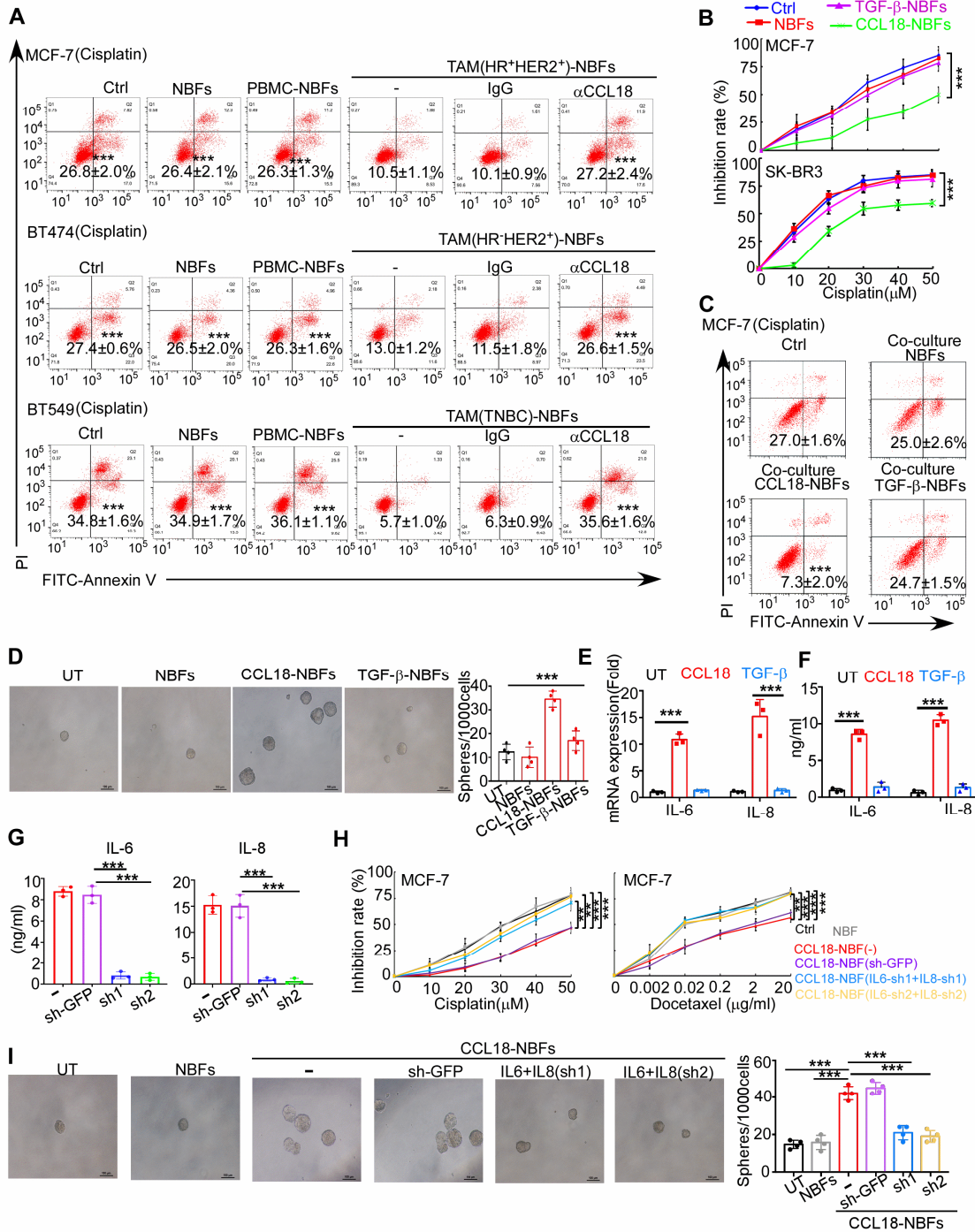
65 **Figure S3. CCL18 produced by TAMs mediates the chemoresistance-inducing**
 66 **phenotype polarization in NBFs, related to Figure 3**

67 **A**, Quantification of Fig.3C: relative α-SMA, FAP, CD10 and GPR77 protein levels in
 68 NBFs with indicated treatment were quantified using ImageJ (n=3). Protein levels were
 69 normalized to GAPDH. **B-C**, Representative immunofluorescent images(**B**) and mean
 70 fluorescent intensity(**C**) for α-SMA and FAP in NBFs with indicated treatment (n=3).
 71 Scale bars, 50 μm. **D**, Quantification of Fig.3D: mean fluorescence intensity for CD10

72 and GPR77 in NBFs with indicated treatment. **E**, Quantification of Fig.3E: relative α -
73 SMA, FAP, CD10 and GPR77 protein levels in NBFs cultured alone (UT) or co-
74 cultured with PBMC or TAMs isolated from different subtypes of breast cancer (n=3).
75 **F**, Quantification of Fig.3F: relative α -SMA, FAP, CD10 and GPR77 protein levels in
76 NBFs cultured alone (UT) or co-cultured with PBMC or TAMs pretreated with control
77 IgG or neutralizing antibodies against CCL18 or TGF- β (n=3).
78 Data expressed as mean \pm SEM, *P< 0.05, **P< 0.01, ***P < 0.001 compared with
79 untreated NBFs (**A**, **C-E**) or NBFs co-cultured with untreated TAMs (**F**) by two-tailed
80 one-way ANOVA with Dunnett's multiple comparison test.

81

Fig.S4



82

83 **Figure S4. NBFs activated by CCL18-producing TAMs mediate chemoresistance**

84 **and CSC enrichment by secreting IL-6 and IL-8, related to Figure 4**

85 **A**, The proportion of apoptotic breast cancer cells treated with cisplatin, cultured alone

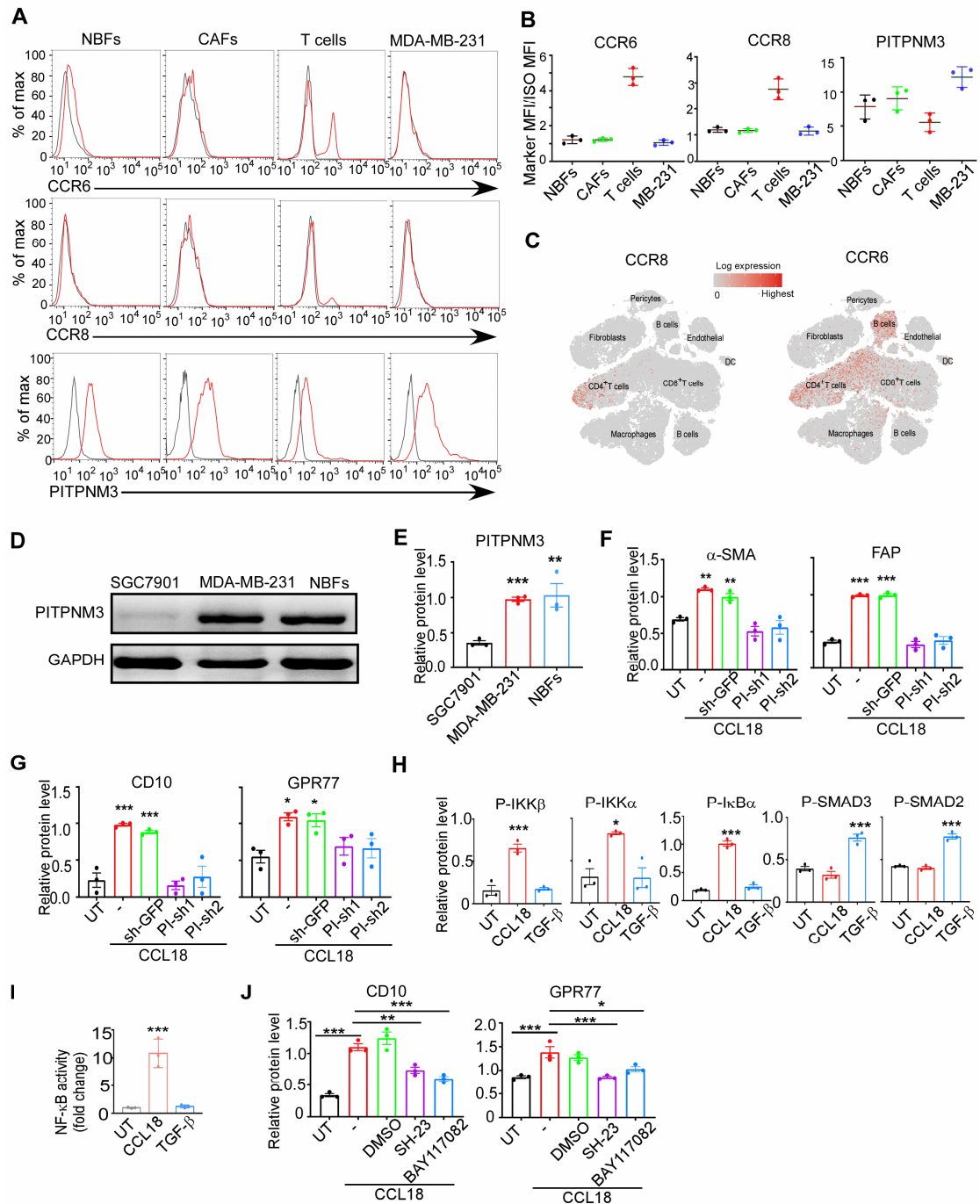
86 (Ctrl) or co-cultured with the fibroblasts with indicated treatment. The proportion of

87 Annexin V⁺/PI⁻ (early apoptosis) and Annexin V⁺/PI⁺ (late apoptosis) cells was shown

88 (n=3). **B**, The growth inhibition rate of cisplatin on MCF-7 (up) and SK-BR3 (down)
89 cells cultured alone (Ctrl) or co-cultured with untreated or CCL18/TGF- β treated NBFs
90 (n=3). **C**, The proportion of apoptotic MCF-7 cells, cultured alone (Ctrl) or co-cultured
91 with indicated fibroblasts, challenged by cisplatin (n=3). **D**, Representative images (left)
92 and quantification(right) of sphere formation in MCF-7 cultured alone or co-cultured
93 with indicated NBFs (n=4). Scale bars, 100 μ m. **E-F**, QRT-PCR(**E**) and ELISA(**F**) for
94 IL-6 and IL-8 in NBFs with indicated treatment (n=3). **G**, ELISA for IL-6 and IL-8 in
95 MCF-7 cultured alone or co-cultured with untreated or CCL18-treated NBFs
96 transduced with shRNA against GFP, IL-6 and IL-8 (n=3). **H**, The growth inhibition
97 rate of cisplatin (left) and docetaxel (right) on MCF-7 cultured alone or co-cultured
98 with untreated or CCL18-treated NBFs transduced with shRNA against GFP, IL-6 and
99 IL-8 (n=3). **I**, The sphere formation of MCF-7 cells cultured alone or co-cultured with
100 NBFs treated as in **H** (n=3).

101 Data expressed as mean \pm SEM, ***P< 0.001 compared with NBFs co-cultured with
102 untreated TAMs(**A**), untreated NBFs (**B-F**) or CCL18-treated NBFs without
103 transducing (**G-I**) by two-tailed one-way ANOVA with Dunnett's multiple comparison
104 test.

Fig.S5



105

106 **Figure S5. PITPNM3 mediates CCL18-induced fibroblast activation via NF-κB**

107 **signaling, related to Figure 5**

108 **A-B**, Representative flow cytometric analysis(A) and quantification of relative MFI (B)

109 for CCR6, CCR8 and PITPNM3 in NBFs, CAFs, T cells and MDA-MB-231 breast

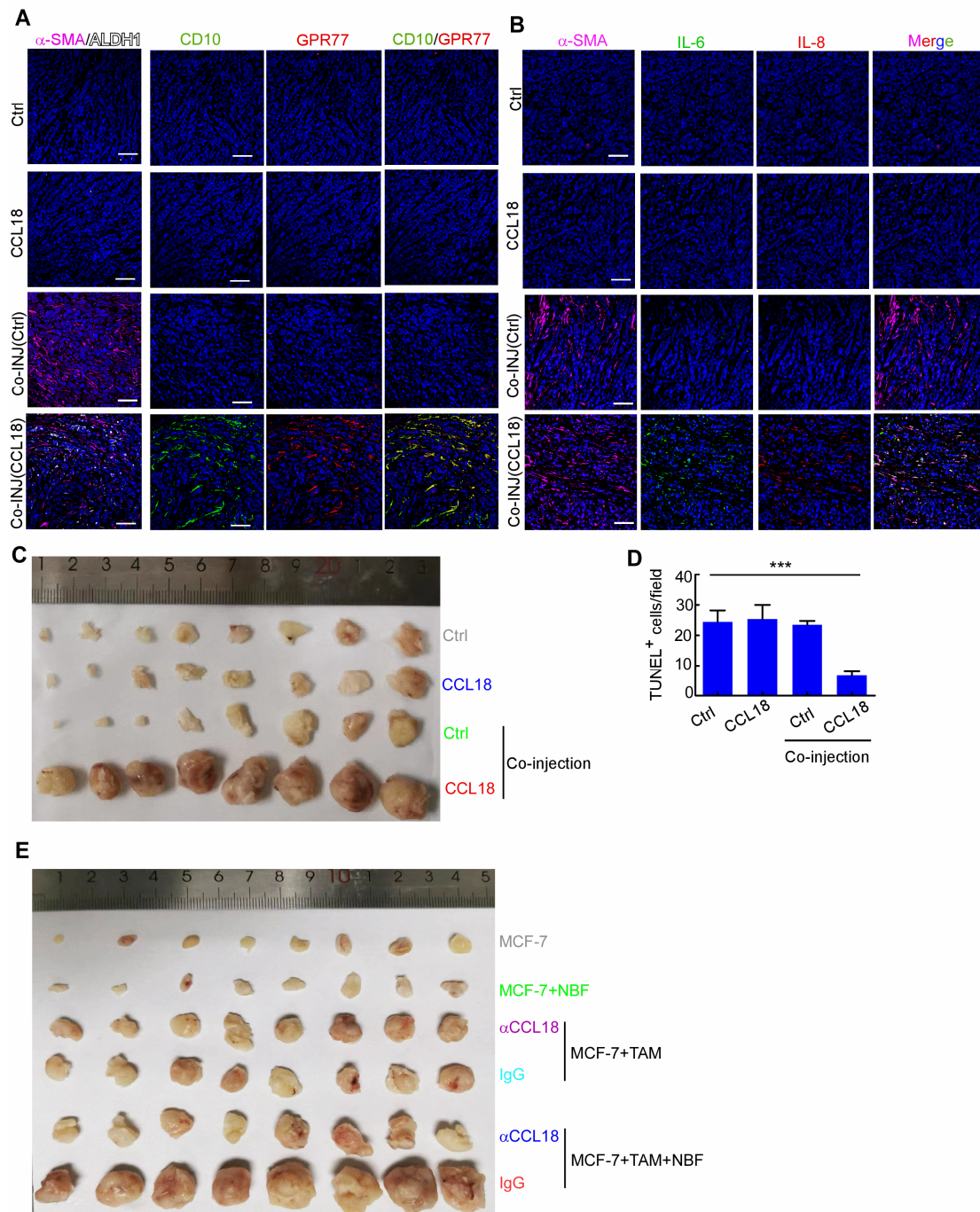
110 cancer cells(n=3). Grey line, isotype. Red line, CCR6/CCR8/PITPNM3. Relative MFI

111 were normalized using isotype MFI as loading control. **C**, Expression plots of CCR6
112 and CCR8 in microenvironment populations derived from scRNA-seq transcriptomes
113 data were exhibited by t-SNE layout. **D-E**, Representative western blotting (**D**) and
114 quantification (**E**) for the expression of PITPNM3 in NBFs, SGC7901 or MDA-MB-
115 231 (n=3). **F-G**, Quantification of Fig.5A: relative α -SMA(**F**), FAP(**F**), CD10(**G**) and
116 GPR77(**G**) protein levels in untreated or CCL18-treated NBFs transduced with GFP
117 shRNA or PITPNM3 shRNAs (n=3). **H**, Quantification of Fig.5C: relative levels of
118 phosphorylated IKK β , IKK α , I κ B α , SMAD2 and SMAD3 in NBFs with indicated
119 treatment was quantified using ImageJ (n=3). Protein levels were normalized to
120 GAPDH. **I**, Luciferase reporter assays for NF- κ B activity in NBFs with indicated
121 treatment (n=3). **J**, Quantification of Fig.5G: relative CD10 and GPR77 protein levels
122 in untreated (UT) or CCL18-activated NBFs treated with DMSO, JSH-23 or
123 BAY117082 (n=3).

124 Data expressed as Mean \pm SEM, *P< 0.05, **P< 0.01, ***P < 0.001 compared with
125 SGC7901(**E**), untreated NBFs(**F-I**) or untreated CCL18-activated NBFs (**J**) by two-
126 tailed one-way ANOVA with Dunnett's multiple comparison test.

127

Fig.S6



128

129 **Figure S6. CCL18 promotes breast cancer tumorigenesis and chemoresistance in**
130 **vivo by activating NBFs, related to Figure 6**

131 **A-B**, Representative immunofluorescent images for (A) α -SMA, ALDH1, CD10 and

132 GPR77, (B) α -SMA, IL6 and IL8 in the harvested xenografts related to Fig.6A-C. Scale

133 bars, 50 μ m. C, Picture of the harvested xenografts related to Fig.6D (n=8 per group).

134 **D**, Quantification for TUNEL⁺ cells in the xenografts related to Fig.6E (mean \pm SEM,
135 n=8 per group). ***P < 0.001 by two-tailed one-way ANOVA with Dunnett's multiple
136 comparison test. **E**, Picture of the harvested xenografts related to Fig.6F (n=8 per group).
137

138 **Supplementary Tables**

139

140 **Supplementary Table 1. Targeting sequences for shRNA**

Name	shRNA1	shRNA2
PITPNM3	5'-GGGAGAAGUGGCUUCGUAATT-3'	5'-CGCGCAUGAUCCUGCGCAATT-3'
P65	5'-GAGUCAGAUCAGCUCCUAA-3'	5'-GCUAUAACUCGCCUAGUGA-3'
IL-6	5'-CTTCCAATCTGGATTCAAT-3'	5'-CCCAGGAGAAGATTCCAAA-3'
IL-8	5'-GAAGAGGGCTGAGAATTCA-3'	5'-GCCAGATGCAATACAAGAT-3'

141

142 **Supplementary Table 2. Primer sequences for qPT-PCR**

Name	Forward	Reverse
CD10	5'-TGGATCTTGTAAGCAGCCTCA-3'	5'-GCACAACGTCTCCAAGTTGC-3'
GPR77	5'-CTGCTGACCATGTATGCCAG-3'	5'-CGCTGAACCGTAGACCACC-3'
ACTA2	5'-AAAAGACAGCTACGTGGGTGA-3'	5'-GCCATGTTCTATCGGGTACTTC-3'
FAP	5'-ATGAGCTTCCTCGTCCAATTCA3'	5'-AGACCACCAGAGAGCATATTTTG3'
COL1A1	5'-GAGGGCCAAGACGAAGACATC3'	5'-CAGATCACGTCATCGCACAAAC3'
COL3A1	5'-GGAGCTGGCTACTTCTCGC3'	5'-GGGAACATCCTCCTTCAACAG3'
IL-6	5'-AAGCCAGAGCTGTGCAGATGAGTA-3'	5'-TGTCTGCAGCCACTGGTTC-3'
IL-8	5'-ACACTGCGCCAACACAGAAATTA-3'	5'-TTTGCTTGAAGTTTCACTGGCATC-3'
GAPDH	5'-GGAGCGAGATCCCTCCAAAAT-3'	5'-GGCTGTTGTCATACTTCTCATGG-3'

143